



Contents lists available at ScienceDirect

Arabian Journal of Chemistry

journal homepage: www.sciencedirect.com



Original article

Bioactive molecular family construction: Design, optimization and antifungal mechanism study of novel 2-phenylglycine derivatives

Cailong Zhao¹, Hong Zhang¹, Xiaocui Chen, Dandan Song, Kuai Chen, Zhibing Wu*

National Key Laboratory of Green Pesticide, Key Laboratory of Green Pesticide and Agricultural Bioengineering, Ministry of Education, Center for R&D of Fine Chemicals of Guizhou University, Guiyang 550025, China

ARTICLE INFO

Article history:

Received 20 March 2023

Accepted 8 October 2023

Available online 11 October 2023

Keywords:

Structural derivation

Antifungal activity

Mechanism study

Molecular docking

Enzyme activity

ABSTRACT

With the widespread use of fungicides, some problems have also gradually emerged, such as resistance, toxicity and residues. Therefore, to develop novel antifungal pesticides with unique structures, safety and high efficiency, a series of 2-phenylglycine derivatives were designed and synthesized. The bioactivity results revealed good antifungal activity of compound **III₁₁** and boscalid against *Nigrospora oryzae*, and they both effectively inhibited spore germination with EC₅₀ values of 17.3 and 3.1 µg/mL, respectively. An antifungal mechanism study showed that both **III₁₁** and boscalid significantly increased the content of nucleic acids, proteins and MDA, which indicated that they could destroy the integrity of the mycelial cell membrane, thus affecting the normal growth of mycelia. Molecular docking results revealed that **III₁₁** bound with some amino acid residues (SER-39, ARG-14 and ARG-43) of succinate dehydrogenase (SDH) through a unique mode involving hydrogen bonds, different from the binding mode of boscalid. Further investigation demonstrated that **III₁₁** exhibited moderate inhibitory activity against SDH (IC₅₀ = 54.5 µg/mL), weaker than that of boscalid (IC₅₀ = 10.7 µg/mL). The results provided sufficient support for the optimization and derivatization of 2-phenylglycine derivatives, which could be further developed and designed as potential fungicides.

© 2023 The Author(s). Published by Elsevier B.V. on behalf of King Saud University. This is an open access article under the CC BY-NC-ND license (<http://creativecommons.org/licenses/by-nc-nd/4.0/>).

1. Introduction

The safety of food and economic crops is closely related to people's livelihood, but the increasing severity and scale of fungal diseases poses a serious threat to global food production and safety

Abbreviations: ¹H NMR, ¹H nuclear magnetic resonance; ¹³C NMR, ¹³C nuclear magnetic resonance; ¹⁹F NMR, ¹⁹F nuclear magnetic resonance; HRMS, high-resolution mass spectrometry; r.t., room temperature; EC₅₀, median effective concentration; IC₅₀, median inhibition concentration; CK, blank control; SEM, scanning electron microscope; FM, fluorescence microscope; PBS, phosphate buffer saline; PDA, potato dextrose agar; PDB, potato dextrose broth; TLC, thin layer chromatography; EA, ethyl acetate; PE, petroleum ether; DCM, dichloromethane; SDH, succinate dehydrogenase; PI, propidium iodide; MDA, malondialdehyde; SD, standard deviation; OD, optical density; SAR, structure-activity relationship.

* Corresponding author.

E-mail address: zbwu@gzu.edu.cn (Z. Wu).

¹ Cailong Zhao and Hong Zhang should be considered joint first author.

Peer review under responsibility of King Saud University.



(Sun et al., 2022; Ray et al., 2017; Li et al., 2021; Fisher et al., 2012). At present, chemical control is still one of the most effective methods to prevent and control fungal diseases because of its low cost, high efficiency and convenience. Accompanying this, the risks of food security and fungicide resistance are also increasing (Chen et al., 2020; Bojarski and Witeska, 2020), and fungal disease control is facing considerable challenges. Therefore, there is an urgent need to continuously develop structurally unique, safe and efficient fungicides to address the growing food security problems.

1,3,4-Oxadiazole, a five-membered heterocyclic ring composed of carbon, nitrogen and oxygen atoms (Wang et al., 2021) with unique electron-rich properties, has been widely used in pharmaceuticals and pesticides and exhibits a wide range of biological activities, including antifungal (Zheng et al., 2017; Wang et al., 2019), insecticidal (Wang et al., 2019), anti-allergic (Guda et al., 2013), anti-inflammatory (Kumar et al., 2021), antibacterial (Xiang et al., 2020), and anti-convulsant activities (Fig. 1) (Harish et al., 2013). In addition, amide, widely found in natural products, is an essential structural unit and active pharmacophore skeleton in drug development (Yao et al., 2017) and has been widely used in pesticides, including fungicides (Esteve-Turrillas et al., 2017), insecticides (Li et al., 2023) and herbicides (Doležalová et al., 2020). It is worth noting that the acylhydrazone and sulfonamide

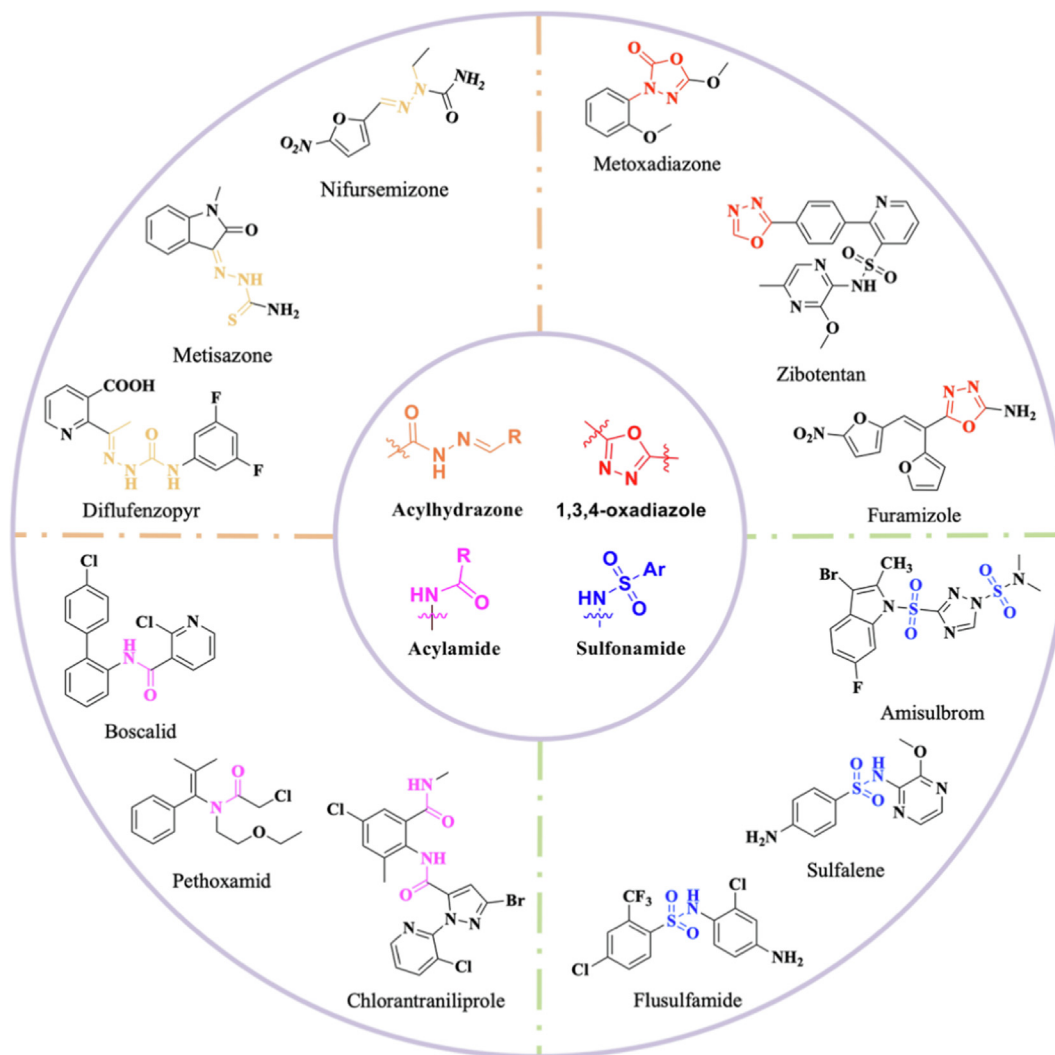


Fig. 1. Commercialized drugs containing 1,3,4-oxadiazole, amide, acylhydrazone and sulfonamide moieties.

structures are similar to the amide structure, which is also an efficient pharmacophore. A variety of commercialized drugs have been developed, such as flusulfamide, sulfalene, siflufenzopyr and nifursemizone (Kalli and Velmurugan, 2022; Zhang et al., 2022; Osmaniye et al., 2018; Iliev et al., 2019).

In our previous work (Zhang et al., 2023), a series of 2-phenylglycine derivatives containing a 1,3,4-oxadiazole moiety with certain inhibitory activity against fungi, bacteria and TMV was reported. In this work, a series of novel 2-phenylglycine derivatives containing 1,3,4-oxadiazole, acylhydrazone and sulfonamide fragments were designed and synthesized to construct a new bioactive molecular family (Fig. 2). The antifungal activity against eight plant pathogenic fungi was evaluated, and the antifungal mechanism of the active compound was explored through morphological observation, quantitative analysis of mycelial growth and a cell membrane integrity study, which provided sufficient support for further development of amino acid derivatives.

2. Materials and methods

2.1. Instruments and chemicals

^1H NMR, ^{13}C NMR and ^{19}F NMR data were measured by a Bruker 400 NMR spectrometer (Bruker Corporation, Germany) using CDCl_3 and $\text{DMSO } d_6$ as solvents. HRMS data were measured by a Thermo

Scientific Q Exactive high resolution mass spectrometer (Thermo Scientific, USA). The melting point was measured by an X-4B melting point meter (Nanbei Instrument Limited, China) and was uncorrected. Spore germination was observed by an Olympus-CX33 microscope (Olympus Co., Ltd., Japan). The mycelial morphology was observed using an Olympus-BX53 FM (Olympus Ltd, Japan) and a Nova Nano SEM450 (Thermo Fisher Scientific, USA). MDA and cellular contents (nucleic acids and proteins) were detected by a CytationTM5 multimode reader (BioTek Instruments, Inc. USA). All reagents and solvents were used directly without further purification or drying after purchase.

2.2. Fungi

F. proliferatum, *G. zeae*, *T. cucumeris*, *A. solani*, *N. oryzae*, *S. sclerotiorum*, and *F. oxysporum* were purchased from Beijing Beina Chuanglian Biotechnology Institute, China; *C. camelliae* was provided by Guizhou Academy of Agricultural Sciences and identified at Sangon Biotech (Shanghai) Co., Ltd., China. All fungi were grown on PDA plates at 25 ± 1 °C and maintained at 4 °C.

2.3. Synthesis

Intermediates **A**, **B**, **C**, **D**, and **E** were synthesized according to the method reported in our previous work (Zhang et al., 2023).

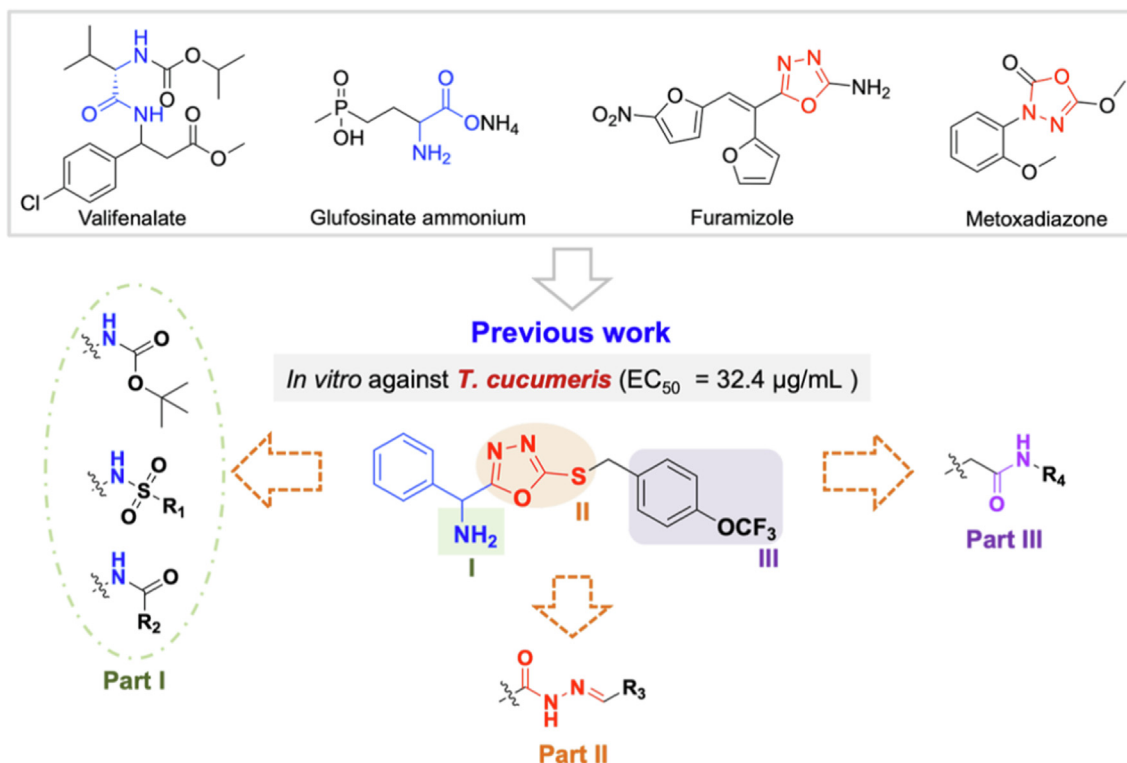


Fig. 2. Molecular design strategy of the target compounds.

2.3.1. General synthesis procedure for F_n intermediates (using F_3 as an example)

Intermediate **B** (3.0 mmol), DMF (8.0 mL), 2-fluorobenzoic acid (3.3 mmol), DPPA (3.6 mmol) and triethylamine (6.7 mmol) were added in turn to a 50 mL round-bottom flask (Shioiri et al., 2022), stirred in an ice bath for 2 h, and then reacted at r.t. The reaction process was monitored by TLC. Then the crude product was extracted with EA and purified by column chromatography (eluent: PE/EA = 30/1) to obtain F_3 , a light yellow solid, with a yield of 83% and an m.p. of 91–93 °C. The synthesis procedures for other intermediates were similar to those for F_3 .

2.3.2. General synthesis procedure for G_n intermediates (using G_3 as an example)

A mixture of F_3 (10.0 mmol), methanol (10.0 mL) and 80% hydrazine hydrate (100.0 mmol) was stirred at 100 °C for 7 h and monitored by TLC (Makane et al., 2019). Subsequently, methanol was removed by vacuum distillation. Then, the crude product was extracted with DCM and purified by column chromatography (eluent: DCM/methanol (MeOH) = 50/1) to obtain G_3 , a white solid, with a yield of 88% and an m.p. of 122–123 °C. The synthesis of other intermediates was similar to that of G_3 .

2.3.3. General synthesis procedure for H_n intermediates (using H_{11} as an example)

4-Aminobenzotrifluoride (10.8 mmol), tetrahydrofuran (10.0 mL), triethylamine (12.9 mmol) and bromoacetyl bromide (12.9 mmol) were added in turn to a 50 mL round-bottom flask and stirred in an ice bath (Kumar et al., 2012). The reaction process was monitored by TLC. Subsequently, tetrahydrofuran was removed by vacuum distillation. Then, the crude product was extracted with DCM and purified by column chromatography (eluent: PE/EA = 30/1) to obtain H_{11} , a white solid, with a yield of 84% and an m.p. of 151–153 °C. The synthesis of other intermediates was to that of H_{11} .

2.3.4. General synthesis procedure for target compounds I_1 – I_6

Intermediate **D** (4.0 mmol), acetonitrile (10.0 mL), water (10.0 mL), potassium carbonate (6.0 mmol) and halogenated compounds (5.0 mmol) were added in turn to a 50 mL round-bottom flask and stirred at r.t. for 7 h (Wang et al., 2021). Then, the crude product was extracted with EA and purified by column chromatography (eluent: PE/EA = 10/1) to obtain target compounds I_1 – I_6 .

2.3.5. General synthesis procedure for target compounds I_7 – I_{14}

Intermediate **E** (1.0 mmol), DCM (8.0 mL), substituted sulfonylchloride (2.0 mmol) and triethylamine (1.0 mol) were added in turn to a 50 mL round-bottom flask and stirred in an ice bath, and the reaction process was monitored by TLC (Wang et al., 2021). Then, the crude product was extracted with DCM and purified by column chromatography (eluent: PE/EA = 30/1) to obtain the target compounds I_7 – I_{14} .

2.3.6. General synthesis procedure for target compounds I_{15} – I_{18}

Intermediate **E** (1.3 mmol), DCM (10.0 mL), EDCI (2.6 mmol), carboxylic acid (1.6 mmol) and DMAP (1.3 mmol) were added in turn to a 50 mL round bottom flask, and the reaction process was monitored by TLC (Li et al., 2016). Then, the crude product was extracted with DCM and purified by column chromatography (eluent: PE/EA = 30/1) to obtain target compounds I_{15} – I_{18} .

2.3.7. General synthesis procedure for target compounds II_1 – II_8

Intermediate **G** (1.8 mmol), ethanol (10.0 mL) and aromatic aldehydes (2.8 mmol) were added in turn to a 50 mL round-bottomed flask and heated for 5 h (Yang et al., 2016). Subsequently, ethanol was removed by vacuum distillation. Then, the crude product was extracted with DCM and purified by column chromatography (eluent: PE/EA = 30/1) to obtain target compounds II_1 – II_4 . Target compounds II_5 – II_8 were synthesized using a similar procedure to that used for II_1 – II_4 .

2.3.8. General synthesis procedure for target compounds **III**₁–**III**₁₃

Intermediate **D** (3.0 mmol), acetone (10.0 mL), sodium bicarbonate (3.0 mmol) and **H**_n (3.0 mmol) were added successively to a 50 mL round bottom flask, and the reaction process was monitored by TLC after heating and refluxing for 7 h (Khanaposhtani et al., 2018). Subsequently, acetone was removed by vacuum distillation. Then, the crude product was extracted with EA and purified by column chromatography (eluent: DCM/EA = 50/1) to obtain the target compounds **III**₁–**III**₁₃.

2.3.9. General synthesis procedure for target compounds **III**₁₄–**III**₁₇

III₄ (1.0 mmol) and DCM (8.0 mL) were added to a 50 mL round-bottom flask. After complete dissolution, trifluoroacetic acid (2.0 mL) was added, the solution was stirred at room temperature for 7 h (Liu et al., 2017), and the pH was adjusted to 8–9 by adding saturated sodium carbonate solution. Then, the crude product was extracted with DCM and purified by column chromatography (eluent: DCM/MeOH = 200/1) to obtain **III**₁₄, a yellow solid, with a yield of 73% and an m.p. of 119–121 °C. The synthesis of other target compounds **III**₁₅–**III**₁₇ was similar to **III**₁₄.

2.4. Bioassay evaluation

2.4.1. *In vitro* antifungal activity bioassay

According to a previously reported method (Wu et al., 2021), all target compounds were preliminarily evaluated for *in vitro* antifungal activity against eight plant pathogenic fungi at a concentration of 50 µg/mL. Sterile distilled water with DMSO (1%) was used as a blank control, and the commercialized fungicide boscalid was used as a positive control. When the mycelia of the blank control group grew to 6 cm, the diameter of the mycelia of the treatment group was recorded, and three replicates were performed for each treatment group. The inhibition rate was calculated according to the formula $I(\%) = [(C - T)/(C - 0.4)] \times 100$, where C is the growth diameter of fungi in the blank control group, T is the diameter of fungi in the treatment group, and I is the inhibition rate. The SD value was calculated as three repeated inhibition data points.

On the basis of *in vitro* antifungal activity, the EC₅₀ values of the compounds with inhibition rates higher than 60% were further determined according to the above method (Zhang et al., 2022). The concentration gradient was 100, 50, 25, 12.5, 6.25, or 3.125 µg/mL, and the linear regression analysis and EC₅₀ values were calculated by SPSS software (version 20.0, IBM).

2.4.2. *In vivo* antifungal activity evaluation

According to the method reported in the literature with some minor modifications (Wang et al., 2019). Rice was used as the testing plant, DMSO (1%) was served as a blank control, and the commercial fungicide boscalid was selected as a positive control. The *in vivo* protective activity of **III**₁₁ against *N. oryzae* was further evaluated. Rice seeds (Xiangliangyou 900) were sown and grown for approximately 8 weeks at r.t. At the tillering stage of rice, 50 mL of **III**₁₁ and boscalid solutions were prepared with Tween 20 and sterile distilled water at 50 µg/mL and 100 µg/mL, respectively. The solutions were sprayed evenly on the rice plants until they were completely moist. After 4 h, the middle part of the rice leaves was ground with sandpaper, and mycelial plugs (diameter 4 mm) were placed on the wounds and fixed with wet cotton. The inoculated plants were then placed in an incubator at 25 °C and 90% relative humidity. At 6 days after inoculation, the lesion length of rice leaves was measured, and the control effect of each treatment group was calculated. The calculation formula is as follows: $I(\%) = (A_0 - A_1)/A_0 \times 100$, where A₀ is the lesion length of the blank control group, and A₁ is the lesion length of the treatment group.

2.4.3. Spore germination of *N. Oryzae*

N. oryzae was inoculated on PDA medium and cultured at 25 °C for approximately 7 to 10 days under the conditions of a 12 h light/12 h dark cycle (Li et al., 2022). The mycelia were washed with sterile distilled water and Tween 20, fully shaken (650 rpm, 15 min), and filtered to obtain a spore suspension. Then, 200 µL of spore suspension was evenly applied to the drug-containing PDA medium and cultured in a constant-temperature incubator at 25 °C for 12 h. Finally, spore germination was observed under a microscope. The total number of spores was not less than 200 in each repeated examination. The total number of spores and spore germination were recorded, and germination was considered to have occurred when the germ tube length reached 1/2 of the spore diameter. DMSO (1%) was used as the blank control, and three replicates were performed for each treatment group. The following formula was used to calculate the spore germination rate: $I = N/M \times 100$, where I represents the inhibition rate, N represents the spore germination number, and M represents the total spore number. The following formula was used to calculate the spore germination inhibition rate: $W = (I_{CK} - I_n)/I_{CK} \times 100$, where W is the spore germination inhibition rate, I_{CK} is the spore germination rate of the control group, and I_n is the spore germination rate of the treatment group; three replicates were performed to obtain the SD value.

2.4.4. Preparation of mycelia of *N. Oryzae*

N. oryzae was cultured on a PDA plate in an incubator at 25 °C for two days, and then fifteen mycelial cakes (diameter 4 mm) were cut from the edge of a normally growing colony and added to a conical flask containing PDB medium. After culturing at 25 °C for 16 h (180 rpm) in a shaker, the residual PDA was removed and transferred to another conical flask containing PDB for additional incubation for 2 days. Finally, the culture was filtered and washed three times with sterile water to obtain the mycelia.

2.5. Mechanism study of the activity of **III**₁₁ against *N. Oryzae*

2.5.1. Morphological observation of the mycelia via SEM

N. oryzae was cultured on a PDA plate for two days, and then five mycelial cakes were cut from the edge of the colony, added to 50 mL PDB medium, and incubated in a shaker at 25 °C and 180 rpm for 36 h. DMSO (1%) was used as a blank control, and solutions of **III**₁₁ and boscalid at different concentrations (25 and 50 µg/mL) were added to the culture medium, which were then incubated under the same conditions for 24 h. Then, the hyphae were washed with PBS buffer (pH = 7.2) three times, fixed with 2.5% glutaraldehyde for more than 12 h, dehydrated with ethanol (30%, 50%, 70%, 90%, and 100%) and *tert*-butanol for 15 min, respectively, dried in a freeze dryer, sprayed with gold, made into a sample, and observed by SEM (Yang et al., 2021).

2.5.2. Morphological observation of the mycelia via FM

Five mycelial cakes were cut from the edge of the normally growing colony and added to the PDB medium. After 36 h of culture in a shaker at 25 °C and 180 rpm, different concentrations of **III**₁₁ and boscalid solutions (0, 25, and 50 µg/mL) were added, and the culture was incubated for 24 h under the same conditions. The hyphae were washed with PBS buffer solution, stained with PI, washed three times with PBS buffer solution after incubation at 37 °C for 15 min, made into samples and observed by FM (Puig et al., 2016).

2.5.3. Determination of dry weight of mycelia

According to the method described in 2.4.4, *N. oryzae* mycelia were cultured in PDB medium in a shaker at 25 °C and 180 rpm

(Mo et al., 2021). Fresh hyphae (0.5 g) were added to 50 mL PDB medium, and then different concentrations of **III₁₁** and boscalid solutions (0, 50, and 100 µg/mL) were added. After 2 days of incubation on a shaker at 25 °C and 180 rpm, the hyphae were filtered and washed three times with equal amounts of distilled water. Ultimately, the samples were dried by vacuum freezing for 6 h, and the hyphae were weighed. Each treatment group was set up with three replications, and the average weight of dry hyphae was recorded as the dry weight of mycelia.

2.5.4. Determination of release cellular contents

0.2 g fresh hyphae (collected in 2.4.4) was suspended in 25 mL sterile water. Then, compound **III₁₁** or boscalid was added to a final concentration of 25 µg/mL (Dou et al., 2022). The obtained samples were cultured in a shaker at 25 °C at a speed of 180 rpm. The absorbance at 260 and 280 nm was measured at 0, 12, 24, 36, 48, 60, and 72 h, respectively.

2.5.5. Determination of MDA content

According to the method described in 2.4.4, the mycelia of *N. oryzae* were cultured on a shaker at 25 °C and 180 rpm for 2 days (Wu et al., 2016). Then, different concentrations of **III₁₁** solutions (0, 25, 50, and 100 µg/mL) were added, and the culture was incubated for 3 days under the same conditions. The hyphae were filtered, washed with an equal amount of distilled water, and then dried by vacuum freezing for 6 h. Finally, the MDA content was determined by an MDA detection kit (Solarbio Technology Co., Ltd., China) according to the instructions, and each treatment group consisted of three replicates.

2.5.6. Molecular docking

Docking analysis was performed using AutoDock Vina 1.1.2 (Du et al., 2021). The protein structure of SDH was downloaded from the PDB database (PDB code: 2FBW). PyMOL 2.3.0 was used to remove the protein-bound water and the original ligand, and the protein structure was imported into Mgttools 1.5.6 for hydrogenation, calculation of charge and merging of nonpolar hydrogen. In addition, the three-dimensional structure of the compound was downloaded from PubChem and then imported into Chemdraw 3D, and the energy was minimized by MM2 to obtain the lowest energy dominant conformation. The two-dimensional binding modes were obtained by Discovery Studio 3.5.

2.5.7. SDH enzyme assay

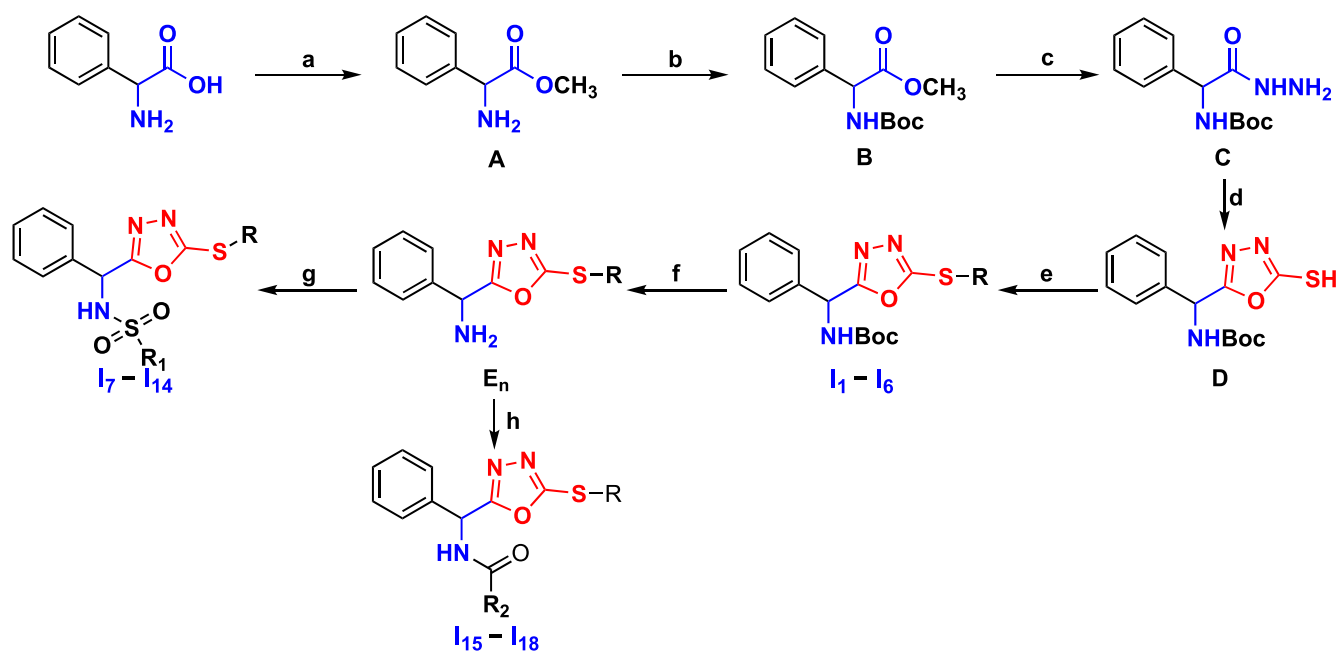
A succinate dehydrogenase assay kit (Suzhou Comin Biotechnology Co., Ltd.) was used to determine the effects of **III₁₁** and boscalid on SDH enzyme activity (Sun et al., 2022). *N. oryzae* was grown in PDB medium for 2 days, and then different concentrations of **III₁₁** and boscalid solutions (0, 6.25, 12.5, 25, 50, 100 and 200 µg/mL) were added, and the culture was incubated at 25 °C for an additional 48 h. Ultimately, the mycelia were filtered and dried by vacuum freezing, and SDH inhibitory activity was detected according to the kit instructions.

Data processing was mainly done by IBM SPSS Statistics 20. And the significant difference analysis using Duncan's test method.

3. Results and discussion

3.1. Chemistry

As shown in Scheme 1, intermediate **C** was obtained by esterification, amino protection and hydrazinolysis, according to our previous work (Zhang et al., 2023). Key intermediate **D** was formed by the reaction of intermediate **C** and carbon disulfide under alkaline conditions. Target compounds **I₁ – I₆** were obtained from intermediate **D**, which reacted with different halogenated compounds by a simple nucleophilic substitution, with a yield range of 69–82%. After removing the protective group of **I_n** intermediates in the presence of trifluoroacetic acid, **E_n** intermediates were obtained. Then, target compounds **I₇ – I₁₄** were synthesized by a substitution reaction of **E_n** and different sulfonyl chlorides, with a yield range of 62–78%; target compounds **I₁₅–I₁₈** were synthesized



Reagents and conditions: (a) H₂SO₄, CH₃OH, reflux, 6 h; (b) (Boc)₂O, CH₃OH, Et₃N, reflux, 7 h; (c) NH₂NH₂·H₂O, CH₃OH, reflux, 6 h; (d) 1. CS₂, KOH, CH₃CH₂OH, r.t., 12 h; 2. reflux, 10 h; (e) RX, K₂CO₃, CH₃CN/H₂O, r.t., 8 h; (f) CF₃COOH, CH₂Cl₂, r.t., overnight; (g) R₁SO₂Cl, Et₃N, CH₂Cl₂, r.t., overnight; (h) R₂COOH, EDCI, DMAP, CH₂Cl₂, r.t., overnight.

Scheme 1. Synthetic route of target compounds **I₁ – I₁₈**.

by a condensation reaction of **E_n** and different acids, with a yield range of 75–82%.

F_n intermediates were obtained by a condensation reaction of **A** and different carboxylic acids in the presence of DPPA at room temperature, with a yield range of 74–83%. **G_n** intermediates were obtained by hydrazinolysis of **F_n** intermediates. Target compounds **II₁ – II₈** were obtained through a reaction of **G_n** intermediates and **C** with aromatic aldehydes, with a yield range of 73–88% (Scheme 2). Target compounds **III₁ – III₁₃** were obtained by a substitution reaction of **D** and **H**, and then **III₁₄ – III₁₇** were obtained by removing the protective group (Scheme 3). All target compounds were identified by ¹H NMR, ¹³C NMR, ¹⁹F NMR and HRMS. The spectral data of target compounds **I₁ – I₁₈**, **II₁ – II₈**, and **III₁ – III₁₇** are provided in the Supporting information.

3.2. Antifungal activity analysis

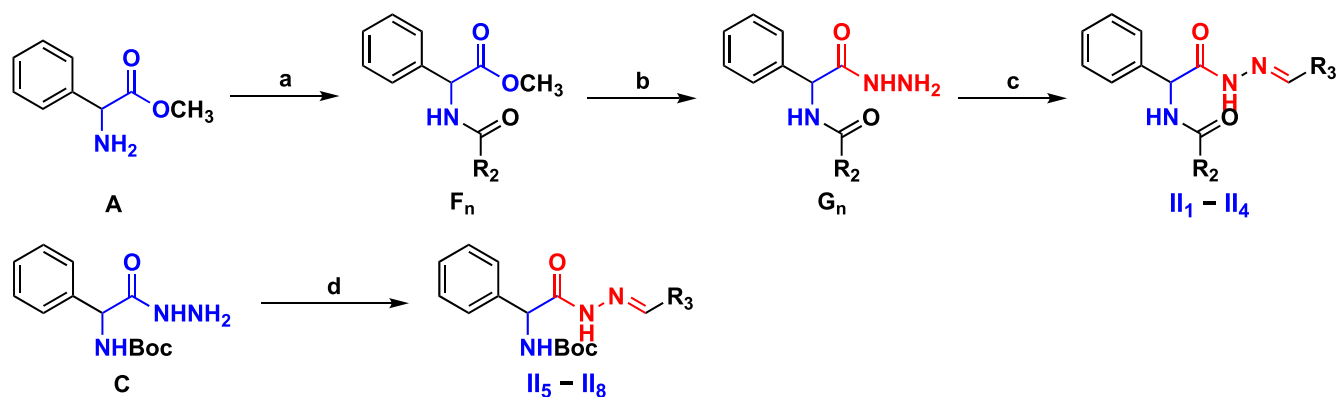
3.2.1. In vitro antifungal activity of target compounds

The antifungal activity of intermediate **D** and all target compounds against eight plant pathogenic fungi (*Fusarium proliferatum*, *Gibberella zeae*, *Thanatephorus cucumeris*, *Alternaria solani*, *Nigros-*

pora oryzae, *Sclerotinia sclerotiorum*, *Fusarium oxysporum*, and *Colletotrichum camelliae*) were evaluated at a concentration of 50 µg/mL. The antifungal results revealed that most target compounds exhibited better activity than that of intermediate **D**. Notably, compound **III₁₁** (81.9%) showed the best activity against *N. oryzae*, which was better than that of intermediate **D** (40.0%) and boscalid (76.3%). Compound **III₁₅** (82.1%) displayed excellent activity against *S. sclerotiorum*, which was far better than that of intermediate **D** (0%) and comparable to that of the commercialized fungicide boscalid (79.4%). Detailed antifungal data are provided in Tables S1–S3 in the Supporting information.

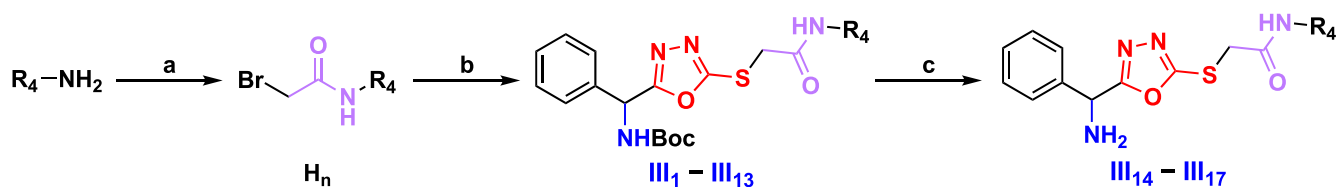
The EC₅₀ values of target compounds with inhibition rates more than 60% were further screened. As shown in Table 1, some target compounds exhibited high antifungal activity by optimizing 2-phenylglycine derivatives. The EC₅₀ values of **I₃** and **III₁₁** against *N. oryzae* were 25.1 and 17.3 µg/mL, respectively. The EC₅₀ values of **III₅** and **III₁₅** against *S. sclerotiorum* were 21.3 and 25.2 µg/mL, respectively, which were significantly improved from intermediate **D**.

Preliminary structure–activity relationship (SAR) analysis demonstrated that the antifungal activity of the target compounds was obviously reduced when 1,3,4-oxadiazole-thioether was



Reagents and conditions: (a) R₂COOH, DPPA, Et₃N, DMF, 0 °C, overnight; (b) NH₂NH₂·H₂O, CH₃OH, refluxing, 6 h; (c) ArCHO, CH₃CH₂OH, refluxing, 5 h; (d) C, ArCHO, CH₃CH₂OH, refluxing, 5 h.

Scheme 2. Synthetic route of target compounds **II₁ – II₈**.



Reagents and conditions: (a) BrCOCH₂Br, Et₃N, CH₂Cl₂, r.t., overnight; (b) **D**, NaHCO₃, acetone, refluxing, 7 h; (c) CF₃COOH, CH₂Cl₂, overnight.

Scheme 3. Synthetic route of the target compounds **III₁ – III₁₇**.

Table 1
EC₅₀ values of some target compounds against *N. oryzae* and *S. sclerotiorum*.^a

No	<i>N. oryzae</i>			No	<i>S. sclerotiorum</i>		
	EC ₅₀ (µg/ml)	regression equation	R ²		EC ₅₀ (µg/ml)	regression equation	R ²
I₃	25.1 ± 0.7	y = 1.6342x + 2.712	0.9881	I₆	107.4 ± 5.1	y = 1.4706x + 2.013	0.8359
I₄	33.5 ± 1.5	y = 1.3131x + 2.9982	0.9897	I₇	29.3 ± 3.5	y = 1.5817x + 2.6794	0.9420
III₂	55.3 ± 3.9	y = 1.4609x + 2.4539	0.9744	I₁₀	61.7 ± 3.6	y = 1.8087x + 1.7617	0.9464
III₄	42.4 ± 2.4	y = 1.1574x + 3.1159	0.9372	I₁₃	34.4 ± 4.2	y = 1.7531x + 2.3055	0.9781
III₇	27.6 ± 1.9	y = 1.0169x + 3.5353	0.9782	III₅	21.3 ± 1.1	y = 1.5766x + 2.9047	0.9806
III₉	40.7 ± 1.0	y = 2.2536x + 1.3728	0.9879	III₁₅	25.2 ± 1.4	y = 1.9103x + 2.3215	0.9986
III₁₁	17.3 ± 0.1	y = 1.5863x + 3.0343	0.9879	BA	2.8 ± 0.1	y = 1.0289x + 4.5455	0.9109
BA	3.1 ± 0.2	y = 0.7420x + 4.6360	0.9524				

^a Values are the means ± SDs of three replicates. BA: boscalid.

replaced by acylhydrazone, as was the case for **II**₁ to **II**₈; however, when 1,3,4-oxadiazole-thioether was retained and the amino and sulfhydryl groups were replaced by organic acids and halogenated hydrocarbons, respectively, the target compounds exhibited better antifungal activity, as was the case for **I**₃ and **III**₁₁. Therefore, 1,3,4-oxadiazole-thioether may be a key functional moiety for the antifungal activity of 2-phenylglycine derivatives.

3.2.2. *In vivo* antifungal activity of **III**₁₁ against *N. Oryzae* on rice leaves

The *in vivo* protective activities of **III**₁₁ and boscalid against *N. oryzae* on rice leaves were 44.3% and 71.0%, respectively, at a concentration of 50 µg/mL. However, the *in vivo* protective activity of **III**₁₁ (65.8%) was increased by approximately 21% at 100 µg/mL,

similar to that of boscalid (76.3%) (Fig. 3). The detailed protective activity data are included in the Supporting information.

3.2.3. Effect of **III**₁₁ treatment on *N. oryzae* spore germination

The germination rates of spores after treatment with **III**₁₁ were 34.9 (25 µg/mL) and 24.6% (50 µg/mL), respectively, which were significantly lower than those of the blank control group (49.0%) (Fig. 4A). Moreover, the inhibition rates of spore germination treated with **III**₁₁ were 28.7% (25 µg/mL) and 49.8% (50 µg/mL), lower than those of boscalid (43.0% and 56.1%) (Fig. 4B). As shown in Fig. 4C to 4E, the spores of *N. oryzae* were treated with different concentrations of **III**₁₁ (25 and 50 µg/mL), and **III**₁₁ significantly reduced the number and length of germ tubes, thereby affecting the spore germination rate. The results demonstrated that **III**₁₁

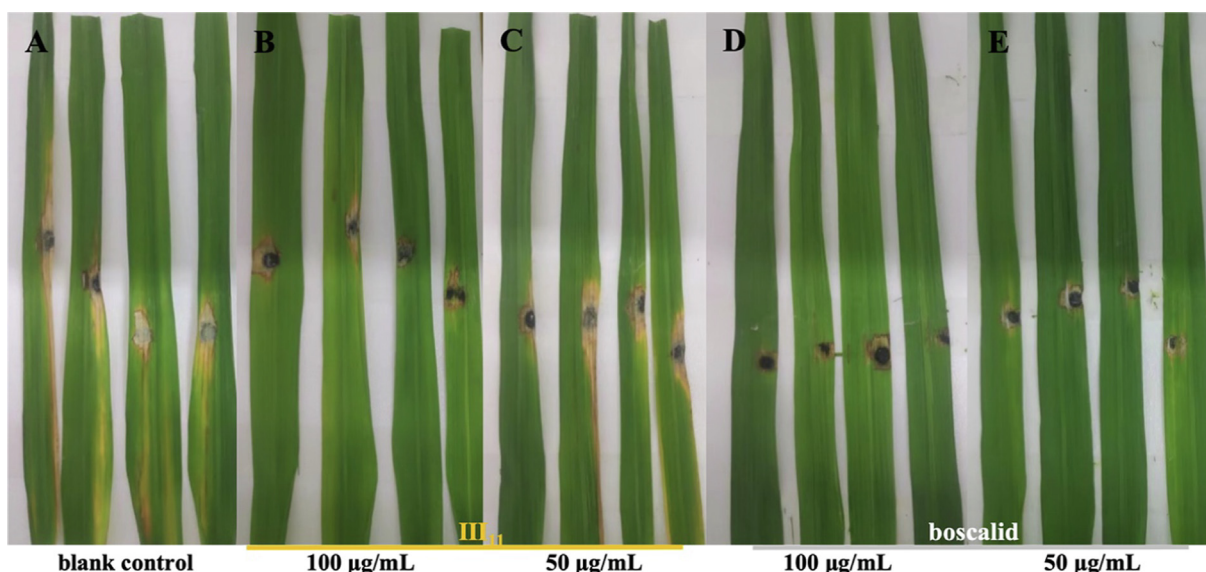


Fig. 3. *In vivo* protective activity against *N. oryzae* on rice leaves. (A) Blank control; (B) and (C) treated with **III**₁₁; (D) and (E) treated with boscalid.

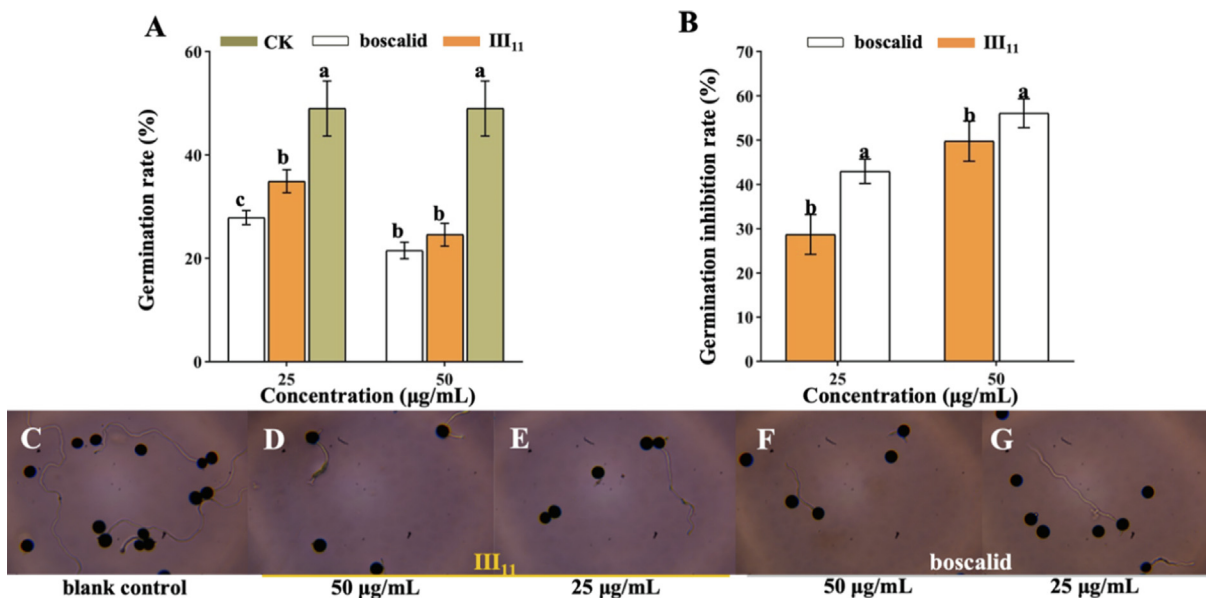


Fig. 4. Effects on spore germination after treatment with **III**₁₁ and boscalid. (A) Spore germination rate; (B) spore germination inhibition rate; from (C) to (E), spore germination after treatment with different compounds for 12 h. Error bars denote the standard error of the mean for three independent experiments. Different lowercase letters in a column indicate significant differences between mean values evaluated by Duncan's multiple range test (*P* less than 0.05).

could inhibit the spore germination of *N. oryzae*, and the inhibition effect was more significant with increasing concentration.

3.3. Preliminary antifungal mechanism against *N. oryzae*

3.3.1. Morphological analysis of *N. Oryzae* via SEM

As shown in Fig. 5A and 5B, the shape of mycelia in the blank control group was normal, full and regular. However, the surface of mycelia became rough and ruptured after treatment with III_{11} at a concentration of 25 $\mu\text{g}/\text{mL}$ (Fig. 5C and 5D). With increasing concentration, the surface was greatly shrunk and the structure was seriously deformed (Fig. 5E and 5F). In addition, more severe shrinkage and damage to the mycelia were observed after treatment with boscalid than after treatment with III_{11} (Fig. 5G, 5H, 5I, and 5J). Boscalid was reported to destroy the structure of mycelia, thus inhibiting the growth of mycelia (Wang et al., 2021). The results demonstrated that III_{11} destroyed the structure of mycelia, and the damage was more obvious with increasing concentration.

3.3.2. Morphological analysis of *N. oryzae* via FM

PI, a nuclear staining reagent, can insert into double-stranded DNA molecules to produce red fluorescence (Zhang et al., 2018). PI cannot pass through the intact cell membrane, but can pass through the damaged cell membrane to stain the nucleus. As shown in Fig. 6A, no red fluorescence was observed in the blank control group, but there was obvious red fluorescence in the mycelia after treatment with III_{11} and boscalid (Fig. 6A, 6B, 6C, and 6D). Moreover, the higher the drug concentration, the more severe the cell membrane damage and the more pronounced the fluorescence. The results revealed that III_{11} destroyed the cell membrane and altered its integrity.

3.3.3. Release of cellular contents of *N. oryzae* treated with III_{11}

The absorbances at 260 and 280 nm were measured by a microplate reader to evaluate the concentrations of nucleic acids and proteins in the mycelial suspensions (Yang et al., 2021). As shown in Fig. 7, the absorbance value of the III_{11} treatment group was sig-

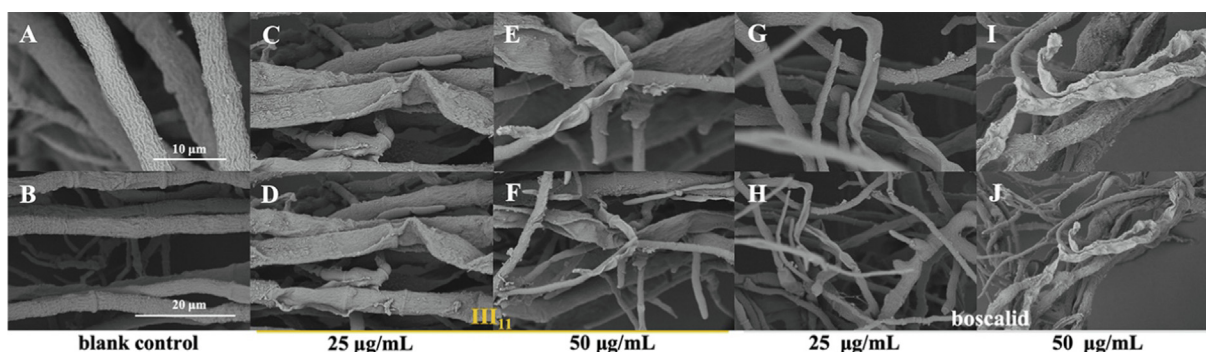


Fig. 5. Morphological observation of *N. oryzae* by SEM. (A) and (B) CK group; (C), (D), (E) and (F) treated with III_{11} ; (G), (H), (I) and (J) treated with boscalid.

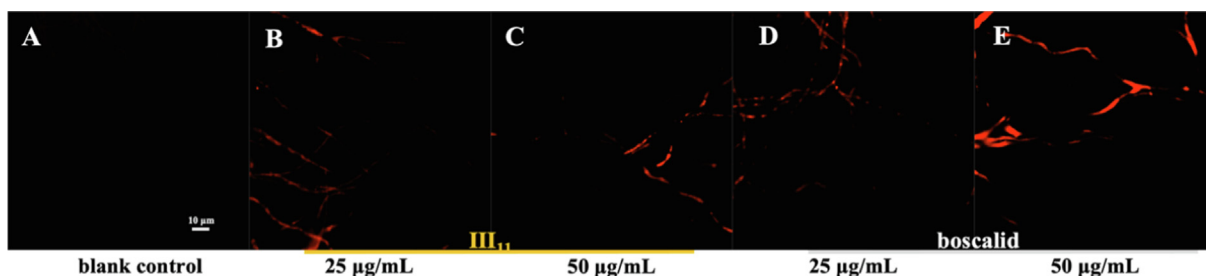


Fig. 6. Morphological observation of *N. oryzae* by FM. (A) CK group; (B) and (C) treated with III_{11} ; (D) and (E) treated with boscalid.

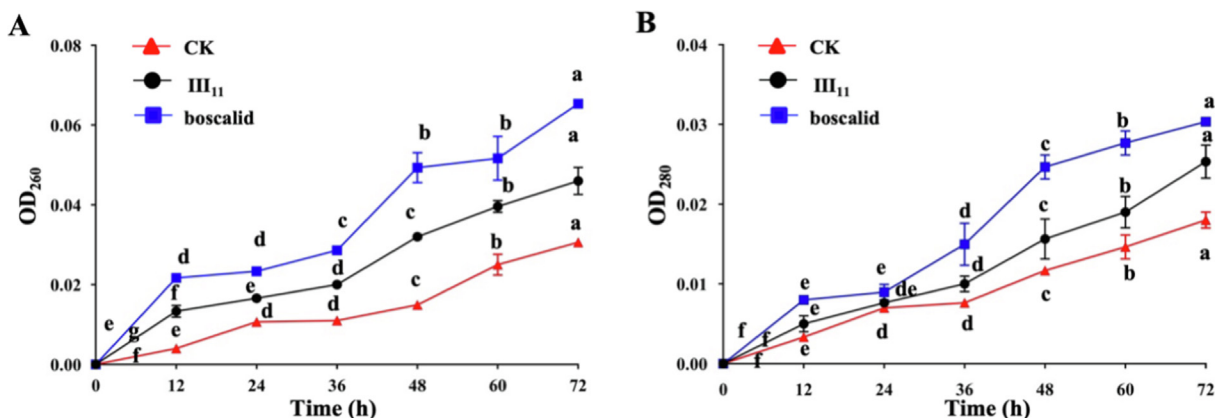


Fig. 7. Released cellular contents of mycelia treated with III_{11} and boscalid at 25 $\mu\text{g}/\text{mL}$. (A) Nucleic acid concentration; (B) protein concentration.

nificantly higher than that of the blank control but slightly lower than that of boscalid treatment group, which indicated significant release of the nucleic acids and proteins of mycelia cells after treatment with **III**₁₁ at 25 $\mu\text{g}/\text{mL}$. We speculated that active molecules may disrupt the cell membrane structure of the mycelia, resulting in the release of cellular contents.

3.3.4. MDA content of *N. oryzae* treated with **III**₁₁

MDA is a product of lipid peroxidation and one of the important indicators to evaluate the integrity of cell membrane structure and function (Yang et al., 2022; Aksakal, 2020). As shown in Fig. 8, following treatment with **III**₁₁ at 25, 50, and 100 $\mu\text{g}/\text{mL}$, the MDA contents were 25.8, 42.3, and 54.8 nmol/g, respectively, which were higher than those of the blank control (18.0 nmol/g). This indicates that **III**₁₁ induces lipid peroxidation in *N. oryzae*, causing

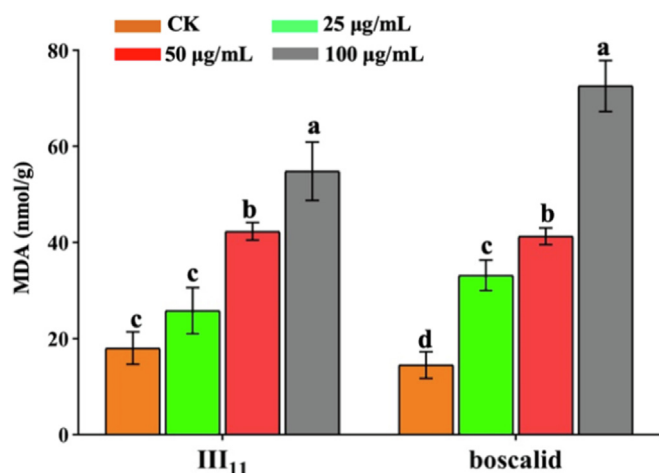


Fig. 8. MDA content of *N. oryzae* treated with **III**₁₁ and boscalid.

membrane damage and thereby altering the integrity of cell membrane structure and function, which supports the findings reported in 2.3.3. The effect of boscalid was better than that of **III**₁₁. Combining the results of SEM and FM revealed that active molecules can destroy the cell membrane structure of the mycelia and release the cellular contents, resulting in inhibition of mycelia growth.

3.3.5. Effect on mycelial growth of *N. oryzae* treated with **III**₁₁

The dry weight of mycelia directly reflects the effect of drugs on mycelial growth (Hou et al., 2018). As shown in Fig. 9, the dry weights of mycelia after treatment with **III**₁₁ and boscalid at 50 $\mu\text{g}/\text{mL}$ were 308.0 and 48.6 mg, respectively, which were both lower than those of the blank control (354.8 mg). Moreover, with increasing concentrations of **III**₁₁ and boscalid, the dry weights of mycelia decreased to 285.5 and 34.2 mg, respectively. The results showed that **III**₁₁ inhibited the growth of *N. oryzae* and reduced the dry weight of mycelia, and the inhibitory effect of boscalid was better than that of compound **III**₁₁.

3.3.6. Molecular docking analysis

In the SAR analysis, both compound **III**₁₁ and boscalid (SDHI) contained amide structures. To explore the potential binding mechanism, molecular docking studies of the ligands **III**₁₁ and boscalid with SDH (PDB code: 2FBW) were performed, and both ligands were found to be effectively embedded in the binding pocket of SDH (Fig. 10). Analysis of the binding mode found that **III**₁₁ formed hydrogen bonds with amino acid residues SER-39, ARG-14 and ARG-43, and the distances of the hydrogen bonds were 3.1, 3.8, and 3.3 Å, respectively. These hydrogen bonds greatly enhance the interaction between the ligands and SDH. Interestingly, as a traditional commercialized SDHI, boscalid only formed a hydrogen bond with HIS-42, and the distance was 3.2 Å. Therefore, it could be speculated that the binding mode of **III**₁₁ was inconsistent with that of boscalid. These results suggest that com-

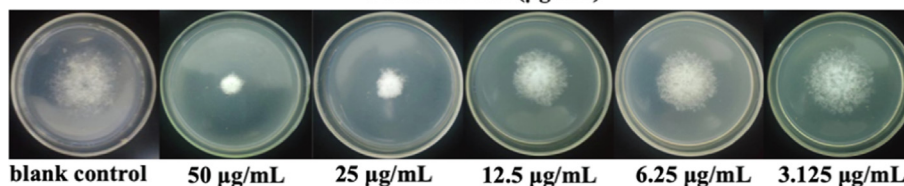
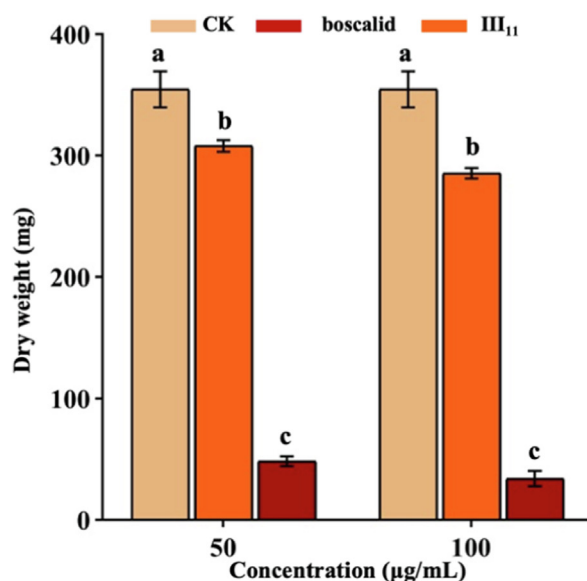


Fig. 9. The dry weight of mycelia treated with **III**₁₁ and boscalid.

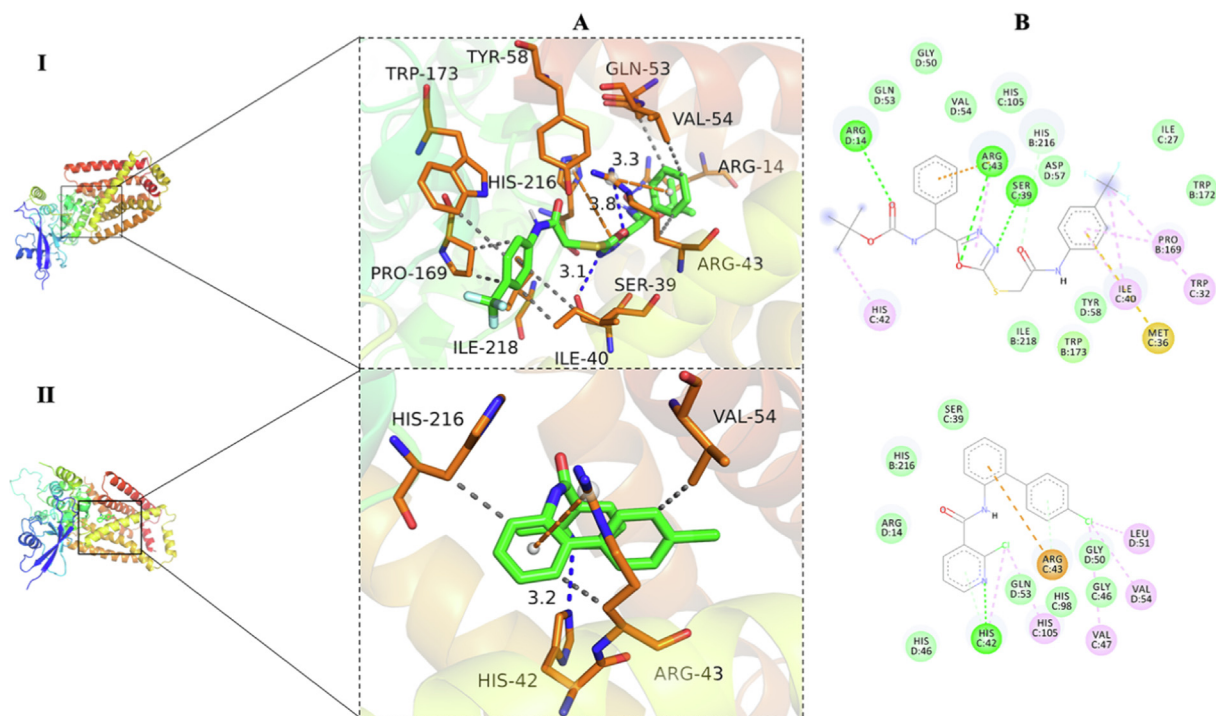


Fig. 10. Molecular docking and binding sites of compound **III₁₁** (I) and boscalid (II) with the SDH protein (PDB code: 2FBW). A: 3D map; B: 2D map.

Table 2
Inhibition of SDH activity by **III₁₁** and boscalid.^a

No	Structure	IC ₅₀ ± SD (μg/mL)	regression equation	R ²
III₁₁		54.5 ± 3.8	y = 1.5944x + 2.2314	0.9085
BA		10.7 ± 1.9	y = 1.3901x + 3.5663	0.9568

^a Values are the means ± SDs of three replicates. BA: boscalid.

compound **III₁₁** is a potential SDHI and deserves further structural optimization and mechanism exploration.

3.3.7. Effects of **III₁₁** treatment on SDH enzymatic activity

As shown in Table 2, compound **III₁₁** exhibited moderate SDH inhibitory activity (IC₅₀ = 54.5 μg/mL), lower than that of boscalid (IC₅₀ = 10.7 μg/mL), which was consistent with the *in vitro* antifungal results.

Although boscalid was reported to destroy the structure of mycelia (Wang et al., 2021), a systematic *in vitro* mechanism study of boscalid and compound **III₁₁** against *N. oryzae* in this work first revealed that both induced lipid peroxidation of cell membranes. This resulted in an increase in MDA content, thereby changing the permeability of cell membranes and causing leakage of intracellular nucleic acids and proteins, thus inhibiting the normal growth of mycelia.

4. Conclusions

In summary, a series of novel 2-phenylglycine derivatives containing 1,3,4-oxadiazole, acylhydrazide and sulfonamide fragments were designed and synthesized to construct a new active molecular family. The bioassay results revealed good antifungal activities of

some compounds against *N. oryzae* and *S. sclerotium*. The EC₅₀ values of **I₃**, **III₇**, **III₁₁**, and boscalid against *N. oryzae* were 25.1, 27.6, 17.3, and 3.1 μg/mL, respectively. An antifungal mechanism study demonstrated that both **III₁₁** and boscalid promoted the peroxide reaction of lipids in the cell membrane and increased the MDA content by acting on mycelial cells. This destroyed the integrity of the cell membrane, resulting in the release of the cellular contents and the inhibition of mycelia growth. In addition, the SDH enzyme activity study showed an inhibitory effect of **III₁₁** on SDH and that **III₁₁** has a unique binding mode with SDH, different from that of boscalid. This is the first systematic report of the inhibitory mechanism of boscalid against *N. oryzae*. These results provided good academic and experimental foundation for the optimization and derivatization of amino acid derivatives and indicate that novel 2-phenylglycine derivatives containing 1,3,4-oxadiazole and amide structures are worthy of further development.

Declaration of competing interest

The authors declare that they have no known competing financial interests or personal relationships that could have appeared to influence the work reported in this paper.

Acknowledgements

This work was supported by the National Natural Science Foundation of China (Nos. 32160655, 21662008), and Breeding Program of Guizhou University (No. 201931).

Appendix A. Supplementary data

Supplementary data to this article can be found online at <https://doi.org/10.1016/j.arabjc.2023.105347>.

References

- Aksakal, F.I., 2020. Evaluation of boscalid toxicity on daphnia magna by using antioxidant enzyme activities, the expression of genes related to antioxidant and detoxification systems, and life-history parameters. *Comp. Biochem. Physiol. C: Toxicol. Pharmacol.* 237. <https://doi.org/10.1016/j.cbpc.2020.108830> 108830.
- Bojarski, B., Witeska, M., 2020. Blood biomarkers of herbicide, insecticide, and fungicide toxicity to fish—a review. *Environ. Sci. Pollut. R.* 27 (16), 19236–19250. <https://doi.org/10.1007/s11356-020-08248-8>.
- Chen, M., Zhang, L.Z., Lu, A.M., Wang, X.B., Si, W.J., Yan, J.H., Yang, C.L., 2020. Novel carboxylated pyrrolone-2-one derivatives bearing a phenylhydrazone moiety: Design, synthesis, antifungal evaluation and 3D-QSAR analysis. *Bioorg. Med. Chem. Lett.* 30, (21). <https://doi.org/10.1016/j.bmcl.2020.127519> 127519.
- Doležalová, I., Petrželová, I., Duchoslav, M., 2020. Selectivity and efficacy of herbicides dimethachlor and pethoxamid in rocket crop. *Plant Protect. Sci.* 56 (4), 305–316. <https://doi.org/10.17221/93/2020-PPS>.
- Dou, L., Shi, H.B., Niu, X., Zhang, H., Zhang, K.K., Wu, Z.B., 2022. Design, synthesis and antifungal mechanism of novel acetophenone derivatives containing 1,3,4-thiadiazole-2-thioethers. *New J. Chem.* 46 (19), 9017–9023. <https://doi.org/10.1039/d2nj01709a>.
- Du, S.Q., Yuan, Q.L., Hu, X.P., Fu, W., Xu, Q., Wei, Z.Y., Xu, J.Z., Shao, X.S., Qian, X.H., 2021. Synthesis and biological activity of novel antifungal leads: 3,5-dichlorobenzyl ester derivatives. *J. Agric. Food Chem.* 69 (51), 15521–15529. <https://doi.org/10.1021/acs.jafc.1c04022>.
- Esteve-Turrillas, F.A., Mercader, J.V., Agulló, C., Abad-Somovilla, A., Abad-Fuentes, A., 2017. Highly sensitive monoclonal antibody-based immunoassays for boscalid analysis in strawberries. *Food Chem.* 267, 2–9. <https://doi.org/10.1016/j.foodchem.2017.06.013>.
- Fisher, M.C., Henk, D.A., Briggs, C.J., Brownstein, J.S., Madoff, L.C., McCraw, S.L., Gurr, S.J., 2012. Emerging fungal threats to animal, plant and ecosystem health. *Nature* 484 (7393), 186–194. <https://doi.org/10.1038/nature10947>.
- Guda, D.R., Park, S.J., Lee, M.W., Kim, T.J., Lee, M.E., 2013. Syntheses and anti-allergic activity of 2-((bis(trimethylsilyl)methylthio)methylsulfonyl)methyl)-5-aryl-1,3,4-oxadiazoles. *Eur. J. Med. Chem.* 62, 84–88. <https://doi.org/10.1016/j.ejmech.2012.12.035>.
- Harish, K.P., Mohana, K.N., Malleth, L., Kumar, B.N.P., 2013. Synthesis of novel 1-[5-(4-methoxy-phenyl)-[1,3,4]oxadiazol-2-yl]-piperazine derivatives and evaluation of their in vivo anticonvulsant activity. *Eur. J. Med. Chem.* 65, 276–283. <https://doi.org/10.1016/j.ejmech.2013.04.054>.
- Hou, Y.P., Mao, X.W., Qu, X.P., Wang, J.X., Chen, C.J., Zhou, M.G., 2018. Molecular and biological characterization of *Sclerotinia sclerotiorum* resistant to the anilino-pyrimidine fungicide cyprodinil. *Pestic. Biochem. Phys.* 146, 80–89. <https://doi.org/10.1016/j.pestbp.2018.09.013>.
- Iliev, I., Kontrec, D., Detcheva, R., Georgieva, M., Balacheva, A., Galic, N., Najpanova, T., 2019. Cancer cell growth inhibition by aroylhydrazones derivatives. *Biotechnol. Biotech. Eq.* 33 (1), 756–763. <https://doi.org/10.1080/13102818.2019.1608302>.
- Kalli, S.B., Velmurugan, V., 2022. Design, synthesis and anti-diabetic activity of piperazine sulphonamide derivatives as dipeptidyl peptidase-4 inhibitors. *Pharmacia* 69 (4), 987–993. <https://doi.org/10.3897/pharmacia.69.e95096>.
- Khanaposhiani, M.M., Rezaei, S., Khalifeh, R., Imanparast, S., Faramarzi, M.A., Bahadorikhalili, S., Safavi, M., Bandarian, F., Esfahani, E.N., Mahdavi, M., Larijan, B., 2018. Design, synthesis, docking study, alpha-glucosidase inhibition, and cytotoxic activities of acridine linked to thioacetamides as novel agents in treatment of type 2 diabetes. *Bioorg. Chem.* 80, 288–295. <https://doi.org/10.1016/j.bioorg.2018.06.035>.
- Kumar, B.R.P., Baig, N.R., Sudhir, S., Kar, K., Kiranmai, M., Pankaj, M., Joghee, N.M., 2012. Discovery of novel gliptazines incorporated with phenylalanine and tyrosine: Synthesis, antidiabetic activity and structure–activity relationships. *Bioorg. Chem.* 45, 12–28. <https://doi.org/10.1016/j.bioorg.2012.08.002>.
- Kumar, D., Kumar, R.R., Pathania, S., Singh, P.K., Kalra, S., Kumar, B., 2021. Investigation of indole functionalized pyrazoles and oxadiazoles as anti-inflammatory agents: Synthesis, in-vivo, in-vitro and in-silico analysis. *Bioorg. Chem.* 114. <https://doi.org/10.1016/j.bioorg.2021.105068> 105068.
- Li, S.K., Li, D.D., Xiao, T.F., Zhang, S.S., Song, Z.H., Ma, H.Y., 2016. Design, synthesis, fungicidal activity, and unexpected docking model of the first chiral boscalid analogues containing oxazolines. *J. Agric. Food Chem.* 64 (46), 8927–8934. <https://doi.org/10.1021/acs.jafc.6b03464>.
- Li, S.Q., Li, X.S., Zhang, H.M., Wang, Z.S., Xu, H.L., 2021. The research progress in and perspective of potential fungicides: Succinate dehydrogenase inhibitors. *Bioorg. Med. Chem.* 50. <https://doi.org/10.1016/j.bmc.2021.116476> 116476.
- Li, X.J., Tu, M.L., Yang, B.X., Zhang, Q.H., Li, H.M., Ma, W., 2023. Chlorantraniliprole in foods: Determination, dissipation and decontamination. *Food Chem.* 406. <https://doi.org/10.1016/j.foodchem.2022.135030> 135030.
- Li, X., Yang, J.K., Jiang, Q.H., Tang, L.J., Xue, Z.W., Wang, H.H., Zhao, D.Y., Miao, J.Q., Liu, X.L., 2022. Baseline sensitivity and control efficacy of a new Qil fungicide, florylpicoxamid, against *Botrytis cinerea*. *Pest Manag. Sci.* 78 (12), 5184–5190. <https://doi.org/10.1002/ps.7137>.
- Liu, Y.X., Wei, Z.L., Liu, Y., Cao, J., Liang, D., Lin, Y.J., Duan, H.F., 2017. Novel alpha-amino acid-derived phase-transfer catalyst application to a highly enantio- and diastereoselective nitro-Mannich reaction. *Org. Biomol. Chem.* 15 (43), 9234–9242. <https://doi.org/10.1039/c7ob02501g>.
- Makane, V.B., Krishna, V.S., Krishna, E.V., Shukla, M., Mahizhaveni, B., Misra, S., Chopra, S., Sriram, D., Dusthacker, V.N.A., Rode, H.B., 2019. Novel 1,3,4-oxadiazoles as antitubercular agents with limited activity against drug-resistant tuberculosis. *Future Med. Chem.* 11 (6), 499–510. <https://doi.org/10.4155/fmc-2018-0378>.
- Mo, F.X., Hu, X.F., Ding, Y., Li, R.Y., Long, Y.H., Wu, X.M., Li, M., 2021. Naturally produced magnolol can significantly damage the plasma membrane of *Rhizoctonia solani*. *Pestic. Biochem. Phys.* 178. <https://doi.org/10.1016/j.pestbp.2021.104942> 104942.
- Osmaniye, D., Levent, S., Karaduman, A.B., Ilgin, S., Özkay, Y., Kaplancıklı, Z.A., 2018. Synthesis of new benzothiazole acylhydrazones as anticancer agents. *Molecules* 23 (5), 1054. <https://doi.org/10.3390/molecules23051054>.
- Puig, M., Moragrega, C., Ruz, L., Calderon, C.E., Cazorla, F.M., Montesinos, E., Llorente, I., 2016. Interaction of antifungal peptide BP15 with stemphylium vesicarium, the causal agent of brown spot of pear. *Fungal Biol-UK* 120 (1), 61–71. <https://doi.org/10.1016/j.funbio.2015.10.007>.
- Ray, M., Ray, A., Dash, S., Mishra, A., Achary, K.G., Nayak, S., Singh, S., 2017. Fungal disease detection in plants: Traditional assays, novel diagnostic techniques and biosensors. *Bioelectron.* 87, 708–723. <https://doi.org/10.1016/j.bios.2016.09.032>.
- Shioiri, T., Ishihara, K., Matsugi, M., 2022. Cutting edge of diphenyl phosphorazidate (DPPA) as a synthetic reagent—A fifty-year odyssey. *Org. Chem. Front.* 9 (12), 3360–3391. <https://doi.org/10.1039/d2qo00403b>.
- Sun, T.G., Jin, X.Y., Zhang, X.M., Lu, X.X., Wang, C.K., Cui, J.L., Xu, H., Yang, X.L., Liu, X.L., Zhang, L., Ling, Y., 2022a. Design, synthesis, and biological activity of novel laccase inhibitors as fungicides against rice blast. *J. Agric. Food Chem.* 70 (45), 14367–14376. <https://doi.org/10.1021/acs.jafc.2c05144>.
- Sun, Y., Yang, Z.H., Liu, Q.S., Sun, X.B., Chen, L.L., Sun, L., Gu, W., 2022b. Design, synthesis, and fungicidal evaluation of novel 1,3-benzodioxole-pyrimidine derivatives as potential succinate dehydrogenase inhibitors. *J. Agric. Food Chem.* 70 (24), 7360–7374. <https://doi.org/10.1021/acs.jafc.2c00734>.
- Wang, J., Ansari, M.F., Zhou, C.H., 2021a. Unique para-aminobenzenesulfonyl oxadiazoles as novel structural potential membrane active antibacterial agents towards drug-resistant methicillin resistant *Staphylococcus aureus*. *Bioorg. Med. Chem. Lett.* 41. <https://doi.org/10.1016/j.bmcl.2021.127995> 127995.
- Wang, S.B., Chen, J.X., Shi, J., Wang, Z.J., Hu, D.Y., Song, B.A., 2021c. Novel cinnamic acid derivatives containing the 1,3,4-oxadiazole moiety: Design, synthesis, antibacterial activities, and mechanisms. *J. Agric. Food Chem.* 69 (40), 11804–11815. <https://doi.org/10.1021/acs.jafc.1c03087>.
- Wang, X.B., Hu, H.R., Zhao, X., Chen, M., Zhang, T.T., Geng, C.W., Mei, Y.D., Lu, A.M., Yang, C.L., 2019a. Novel quinazolin-4(3H)-one derivatives containing a 1,3,4-oxadiazole thioether moiety as potential bactericides and fungicides: Design, synthesis, characterization and 3D-QSAR analysis. *Journal of Saudi Chemical Society*. 23, 1144–1156. <https://doi.org/10.1016/j.jscs.2019.07.006>.
- Wang, X.B., Fu, X.C., Yan, J.H., Wang, A., Wang, M.Q., Chen, M., Yang, C.L., Song, Y.M., 2019c. Design and synthesis of novel 2-(6-thioxo-1,3,5-thiadiazinan-3-yl)-N-phenylacetylhydrazide derivatives as potential fungicides. *Mol. Divers.* 23 (3), 573–583. <https://doi.org/10.1007/s11030-018-9891-7>.
- Wang, W., Zhang, S., Wang, J.H., Wu, F.R., Wang, T., Xu, G., 2021b. Bioactivity-guided synthesis accelerates the discovery of 3-(Isoquinolinyl)-4-chromenones as potent fungicide candidates. *J. Agric. Food Chem.* 69, 491–500. <https://doi.org/10.1021/acs.jafc.0c06700>.
- Wang, J., Zhang, P.L., Ansari, M.F., Li, S., Zhou, C.H., 2021d. Molecular design and preparation of 2-aminothiazole sulfanilamide oxides as membrane active antibacterial agents for drug resistant *Acinetobacter baumannii*. *Bioorg. Chem.* 113. <https://doi.org/10.1016/j.bioorg.2021.105039> 105039.
- Wang, W., Zheng, X.R., Huang, X.Y., Mao, M.Z., Liu, K.Y., Xue, C., Wang, L.P., Ning, B.K., 2019b. Synthesis and insecticidal evaluation of novel N-pyridylpyrazole derivatives containing diacylhydrazine/1,3,4-oxadiazole moieties. *J. Heterocycl. Chem.* 56 (4), 1330–1336. <https://doi.org/10.1002/jhet.3505>.
- Wu, Z.B., Park, H.Y., Xie, D.W., Yang, J.X., Hou, S.T., Shahzad, N., Kim, C.K., Yang, S., 2021. Synthesis, biological evaluation, and 3D-QSAR studies of N-(substituted pyridine-4-yl)-1-(substituted phenyl)-5-trifluoromethyl-1H-pyrazole-4-carboxamide derivatives as potential succinate dehydrogenase inhibitors. *J. Agric. Food Chem.* 69 (4), 1214–1223. <https://doi.org/10.1021/acs.jafc.0c05702>.
- Wu, L., Qiu, Z.H., Zhou, Y., Du, Y.P., Liu, C.N., Ye, J., Hu, X.J., 2016. Physiological effects of the herbicide glyphosate on the cyanobacterium *Microcystis aeruginosa*. *Aquat. Toxicol.* 178, 72–79. <https://doi.org/10.1016/j.aquatox.2016.07.010>.
- Xiang, J., Liu, D.Y., Chen, J.X., Hu, D.Y., Song, B.A., 2020. Design and synthesis of novel 1,3,4-oxadiazole sulfone compounds containing 3,4-dichloroisothiazolylamide

- moieties and evaluation of rice bacterial activity. *Pestic. Biochem. Phys.* 170, <https://doi.org/10.1016/j.pestbp.2020.104695> 104695.
- Yang, Y.D., He, Y.H., Ma, K.Y., Li, H., Zhang, Z.J., Sun, Y., Wang, Y.L., Hu, G.F., Wang, R. X., Liu, Y.Q., 2021a. Design and discovery of novel antifungal quinoline derivatives with acylhydrazide as a promising pharmacophore. *J. Agric. Food Chem.* 69 (30), 8347–8357. <https://doi.org/10.1021/acs.jafc.1c00670>.
- Yang, Z.B., Hu, D.Y., Zeng, S., Song, B.A., 2016. Novel hydrazone derivatives containing pyridine amide moiety: Design, synthesis, and insecticidal activity. *Bioorg. Med. Chem. Lett.* 26 (4), 1161–1164. <https://doi.org/10.1016/j.bmcl.2016.01.047>.
- Yang, Z.H., Sun, Y., Liu, Q.S., Li, A.L., Wang, W.Y., Gu, W., 2021b. Design, synthesis, and antifungal activity of novel thiophene/furan-1,3,4-oxadiazole carboxamides as potent succinate dehydrogenase inhibitors. *J. Agric. Food Chem.* 69 (45), 13373–13385. <https://doi.org/10.1021/acs.jafc.1c03857>.
- Yang, J.X., Xie, D.W., Zhang, C.Z., Zhao, C.L., Wu, Z.B., Xue, W., 2022. Synthesis, antifungal activity and *in vitro* mechanism of novel 1-substituted-5-trifluoromethyl-1H-pyrazole-4-carboxamide derivatives. *Arab. J. Chem.* 15, (8). <https://doi.org/10.1016/j.arabjc.2022.103987> 103987.
- Yao, T.T., Xiao, D.X., Li, Z.S., Cheng, J.L., Fang, S.W., Du, Y.J., Zhao, J.H., Dong, X.W., Zhu, G.N., 2017. Design, synthesis, and fungicidal evaluation of novel pyrazole-furan and pyrazole-pyrrole carboxamide as succinate dehydrogenase inhibitors. *J. Agric. Food Chem.* 65, 5397–5403. <https://doi.org/10.1021/acs.jafc.7b01251>.
- Zhang, N., Fan, Y.X., Li, C., Wang, Q.M., Leksawasdi, N., Li, F.L., Wang, S.A., 2018. Cell permeability and nuclear DNA staining by propidium iodide in basidiomycetous yeasts. *Appl. Microbiol. Biot.* 102 (9), 4183–4191. <https://doi.org/10.1007/s00253-018-8906-8>.
- Zhang, S.G., Wan, Y.Q., Wen, Y., Zhang, W.H., 2022a. Novel coumarin 7-carboxamide/sulfonamide derivatives as potential fungicidal agents: Design, synthesis, and biological evaluation. *Molecules* 27 (20), 6904. <https://doi.org/10.3390/molecules27206904>.
- Zhang, X.M., Xu, H., Su, H.F., Yang, X.L., Sun, T.D., Lu, X.X., Shi, F.S., Duan, H.X., Liu, X. L., Ling, Y., 2022b. Design, synthesis, and biological activity of novel fungicides containing a 1,2,3,4-tetrahydroquinoline scaffold and acting as laccase inhibitors. *J. Agric. Food Chem.* 70 (6), 1776–1787. <https://doi.org/10.1021/acs.jafc.1c06595>.
- Zhang, H., Zhao, C.L., Zheng, H.L., Chen, X.C., Chen, B., Wu, Z.B., 2023. Design, synthesis and bioassay of 2-phenylglycine derivatives as potential pesticide candidates. *Chem. Biodivers.* 20, (1). <https://doi.org/10.1002/cbdv.202200957> e202200957.
- Zheng, Y.T., Zhang, T.T., Wang, P.Y., Wu, Z.B., Zhou, L., Ye, Y.Q., Zhou, X., He, M., Yang, S., 2017. Synthesis and bioactivities of novel 2-(thioether/sulfone)-5-pyrazolyl-1,3,4-oxadiazole derivatives. *Chinese Chem. Lett.* 28 (2), 253–256. <https://doi.org/10.1016/j.ccllet.2016.06.055>.